Equations of Motion of a Deep Submergence Rescue Vehicle with Active Mercury Damping Control

RONALD D. PALAMARA*
Purdue University, Indianapolis, Ind.

AND

WENDELL J. BRIDGES†
Naval Avionics Facility, Indianapolis, Ind.

The six-degree-of-freedom equations of motion are derived for a submerged body capable of dynamic internal mass movement. Simplified vehicle roll characteristics are then analyzed for creeping forward speed and it is shown that internal movement of liquid mercury can be utilized to control dynamically the roll attitude of the vehicle. The results of an analog computer simulation of the complete six-degree-of-freedom equations are cited to verify the simplified roll analysis.

Nomenclature

O'	= inertially fixed point
O	= body fixed point located at the initial position of the center of mass
P	= arbitrary point located on the body
$\mathbf{R}_i$	= position vector of point P relative to point O'
$\mathbf{R}_o$	= position vector of point O relative to point O'
$\mathbf{r}_i$	= position vector of point P relative to point O
$\boldsymbol{\omega}$	= angular velocity of $\mathbf{r}_i$ with respect to inertial space
$[\dot{}]$	= derivative with respect to time in the rotating coordinate system
$\boldsymbol{\alpha}_1, \boldsymbol{\alpha}_2, \boldsymbol{\alpha}_3$	= orthogonal unit vectors of body coordinate system
m_i	= ith particle of mass
m	= mass of body
$\mathbf{r}$	= position vector of the center of mass with respect to point O
$\mathbf{V}_o$	= velocity vector of point O relative to O'
$\mathbf{F}$	= force vector
u,v,w	= components of $\mathbf{V}_o$ along body axes
p,q,r	= components of $\boldsymbol{\omega}$ along body axes
x,y,z	= components of $\mathbf{r}$ along body axes
x_i,y_i,z_i	= components of r_i along body axes
F_1,F_2,F_3	= components of $\mathbf{F}$ along body axes
$\mathbf{H}_o$	= angular momentum vector about point O
I_o	= moment of inertia tensor
I_{xx}, I_{yy}, I_{zz}	= principle moments of inertia
I_{xy}, I_{yz}, I_{xz}	= products of inertia
p	= set of particles within the body with acceleration $[\ddot{\mathbf{r}}]$
p'	= set of particles within the body with velocity $[\dot{\mathbf{r}}]$
$\mathbf{r}_A, \mathbf{r}_V$	= position vectors of the center of mass of p and p', respectively
x_A,y_A,z_A	= components of $\mathbf{r}_A$ along body axes
x_V,y_V,z_V	= components of $\mathbf{r}_V$ along body axes
$(F_1)_{\text{hyd}}, (F_2)_{\text{hyd}}, (F_3)_{\text{hyd}}$	= force components along the body axes due to hydrodynamics forces
K,M,N	= components of torque along the body axes due to hydrodynamic forces
ρ	= density of seawater
l	= characteristic length of the deep submergence rescue vehicle (DSRV)
W	= weight of the DSRV
B	= buoyancy force
φ,θ,ψ	= DSRV roll, pitch, and yaw angles
$\mathbf{r}'$	= position vector from point O to effective point of bouyancy force
x_B,y_B,z_B	= components of $\mathbf{r}'$
F_X,F_Y,F_Z	= components of external force acting on the DSRV along the body axes
$\Sigma K,\Sigma M,\Sigma N$	= components of external torque acting on the DSRV along the body axes
δ_s, δ_r	= shroud angles due to rotation about the DSRV pitch and yaw axes, respectively
X_{ij}, Y_{ij}, Z_{ij}	= hydrodynamic force coefficients
K_{ij}, M_{ij}, N_{ij}	= hydrodynamic moment coefficients
W_N	= DSRV roll natural frequency
DR	= DSRV roll damping ratio
Z_B	= distance between initial position of the DSRV center of mass and the effective location of the buoyancy force
b_1,b_2,b_3	= simplified roll transfer function coefficients
W_{Hg}	= weight difference of the mercury in the roll trim tanks
φ_f	= roll control feedback signal
K	= roll control loop gain
γ	= specific weight of mercury
A	= cross-sectional area of the mercury transfer tube
$Z_1 - Z_2$	= height change in the mercury storage tanks
L	= length of mercury transfer tube
f_1	= friction factor of mercury transfer tube
D	= diameter of mercury transfer tube
A'	= cross-sectional area of mercury storage tanks
δP	= accumulator pressure difference
Ω_N	= oscillation frequency in mercury system
Z	= displacement of mercury in the transfer tube
$\dot{W}_{\text{Hg}}$	= mass flow rate in mercury system
t_m	= time to reach maximum mass flow rate

Presented at AIAA-ONR Symposium on Deep Submergence Propulsion and Marine Systems, Forest Park, Ill., February 28–March 1, 1966; received May 29, 1967; revision received October 27, 1967.

* Control Systems Consultant and Assistant Professor, Mechanical Engineering, Indianapolis campus. Associate Member AIAA.

† Control Systems Engineer.

Introduction

THE problem of mating a deep submergence rescue vehicle (DSRV) to the hatch of an immobile submarine is similar in many facets to the task faced by the Gemini vehicles during the terminal phase of rendezvous. To rendezvous successfully with another satellite, the Gemini must be controlled in roll, pitch, and yaw as well as velocity along three body axes.

The DSRV, like the Gemini vehicle, is a six-degree-of-freedom vehicle. The need for six-degree-of-freedom control, manual and automatic, is justified when one considers the undesirable environmental factors of impaired visibility and perturbing cross currents present during the delicate mating maneuver. In order to achieve a mating of the DSRV to the distressed submarine, strictly from a mechanics viewpoint, the DSRV must be capable of 1) translating at cruise velocity to the vicinity of the distressed submarine, 2) translating at hover speed to the location of the hatch of the distressed submarine, 3) matching the attitude of its mating skirt to that of the hatch, and 4) performing the final phase of translational positioning until a "skirt-hatch" seal is affected.

In order to perform translation, the vehicle is equipped with three-axes thrust, supplied by a main propeller along the vehicle longitudinal axis and auxiliary thrusters perpendicular to the vehicle longitudinal axis. Attitude control is achieved with a shroud, auxiliary thrusters, and a mercury trim system. The main propeller is enclosed with a truncated conical shroud which can be rotated into the main prop flow to produce pitch and yaw rotations about body axes. In addition, the auxiliary thrusters can yield moments about both the y and z axes of the vehicle. In order to achieve a static rotation about the vehicle's pitch or roll axes, the DSRV is provided with a supply of mercury that can be used to produce couple moments by moving the center of mass along either the vehicle's pitch or roll axis. The following modes of applying torques to the vehicle are then available: 1) pitch—auxiliary thrusters, shroud, static mercury trim; 2) yaw—auxiliary thrusters, shroud; and 3) roll—static mercury trim. With these modes the vehicle has no form of dynamic roll control. The obvious solution for achieving dynamic roll control would be to add another set of auxiliary thrusters about the vehicle roll axis. However, another method, which would utilize the existing controls, would be to use the mercury trim system as a source of dynamic roll damping. If the dynamic motion of the mercury can be controlled satisfactorily within the bounds dictated by the natural frequency of the vehicle, the necessity for additional auxiliary thrusters would be removed. Such a method of internal mass movement, used to achieve dynamic attitude control in roll, is investigated and reported herein.

Procedure and Assumptions

The approach was to derive the six-degree-of-freedom equations of motion for a body capable of internal mass movement. The hydrodynamic forces and moments used were those initially reported in Ref. 1, and were revised as new experimental data became available. The dynamic equations are valid for the translation cruise and translation hover maneuvers. Matching the attitude of mating skirt and hatch and performing the final seal is not discussed herein, but is treated in detail in Ref. 2. The effect of perturbing flowfields is also omitted from the equations, but is discussed in Ref. 3 for determining the minimum-time flight paths to the distressed submarine.

To determine roll characteristics, the equations were linearized and motion described in the horizontal plane. This simplified model was then used to determine necessary control system requirements for satisfactory stability and performance using standard linear techniques and an analog simulation of the constrained motion in the horizontal plane.

Fig. 1 Vector diagram for moment equations.

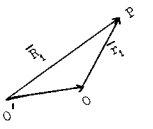

This analysis was followed by a complete six-degree-of-freedom simulation of the full nonlinear equations to insure that the mercury roll control system synthesized for the linear vehicle dynamics was adequate for controlling the unconstrained vehicle. Further discussion of the six-degree-of-freedom-simulation is given in Ref. 4.

Kinematic Equations and External Loadings

A. Force Equations

Choosing an inertially fixed point O' and a point O, fixed in the body at an initial position of the center of mass, then a point P on the body (see Fig. 1) is located by $\mathbf{R}_i = \mathbf{R}_o + \mathbf{r}_i$. If a body fixed coordinate system $\boldsymbol{\alpha}_i$ is placed at point O, the velocity and acceleration of point P, with respect to O' but measured in the body fixed frame, are

$$\dot{\mathbf{R}}_i = \dot{\mathbf{R}}_o + [\dot{\mathbf{r}}_i] + \boldsymbol{\omega} \times \mathbf{r}_i$$

$$\ddot{\mathbf{R}}_i = \ddot{\mathbf{R}}_o + [\ddot{\mathbf{r}}_i] + 2\boldsymbol{\omega} \times [\dot{\mathbf{r}}] + \boldsymbol{\omega} \times (\boldsymbol{\omega} \times \mathbf{r}_i) + \dot{\boldsymbol{\omega}} \times \mathbf{r}_i$$

The external forces acting on the entire body are equal to the rate of change of the linear momentum of all m_i particles of the body;

$$\mathbf{F} = \lambda m_i \ddot{\mathbf{R}}_o + \Sigma m_i[\ddot{\mathbf{r}}_i] + 2\Sigma m_i(\boldsymbol{\omega} \times [\dot{\mathbf{r}}_i]) + \Sigma\boldsymbol{\omega} \times (\boldsymbol{\omega} \times m_i\mathbf{r}_i) + \Sigma(\dot{\boldsymbol{\omega}} \times m_i\mathbf{r}_i) \quad (1)$$

Now, defining the following quantities:

center of mass

$$\mathbf{r} = \Sigma m_i r_i/\Sigma m_i = \Sigma m_i r_i/m$$

velocity of mass center with respect to o as seen from $\boldsymbol{\alpha}_i$ frame

$$[\dot{\mathbf{r}}] = \Sigma m_i[\dot{\mathbf{r}}_i]/\Sigma m_i$$

acceleration of mass center with respect to O

$$[\ddot{\mathbf{r}}] = \Sigma m_i[\ddot{\mathbf{r}}_i]/\Sigma m_i$$

acceleration of origin in body fixed coordinates

$$\ddot{\mathbf{R}}_o = [\dot{\mathbf{V}}_o] + \boldsymbol{\omega} \times \mathbf{V}_o$$

and substituting these definitions into (1),

$$\mathbf{F} = m[\dot{\mathbf{V}}_o] + m(\boldsymbol{\omega} \times \mathbf{V}_o) + 2m(\boldsymbol{\omega} \times [\dot{\mathbf{r}}]) + \boldsymbol{\omega} \times (\boldsymbol{\omega} \times m\mathbf{r}) + \dot{\boldsymbol{\omega}} \times m\mathbf{r} + m[\ddot{\mathbf{r}}] \quad (2)$$

Then by expressing the scalar components of these vectors along the $\boldsymbol{\alpha}_i$ body frame, the scalar force equations can be obtained.

The vector equations along $\boldsymbol{\alpha}_i$ are

$$\mathbf{V}_o = u\boldsymbol{\alpha}_1 + v\boldsymbol{\alpha}_2 + w\boldsymbol{\alpha}_3 \qquad \boldsymbol{\omega} = p\boldsymbol{\alpha}_1 + q\boldsymbol{\alpha}_2 + r\boldsymbol{\alpha}_3$$

$$\mathbf{r} = x\boldsymbol{\alpha}_1 + y\boldsymbol{\alpha}_2 + z\boldsymbol{\alpha}_3 \qquad [\dot{\mathbf{r}}] = \dot{x}\boldsymbol{\alpha}_1 + \dot{y}\boldsymbol{\alpha}_2 + \dot{z}\boldsymbol{\alpha}_3$$

$$[\ddot{\mathbf{r}}] = \ddot{x}\boldsymbol{\alpha}_1 + \ddot{y}\boldsymbol{\alpha}_2 + \ddot{z}\boldsymbol{\alpha}_3 \qquad \mathbf{F} = F_1\boldsymbol{\alpha}_1 + F_2\boldsymbol{\alpha}_2 + F_3\boldsymbol{\alpha}_3$$

Substituting into (2),

$$F_1 = m(\dot{u} + qw - rv) - mx(r^2 + q^2) + my(pq - \dot{r}) + mz(\dot{q} + pr) + 2m(q\dot{z} - r\dot{y}) + m\ddot{x} \quad (3)$$

$$F_2 = m(\dot{v} + ru - pw) - my(r^2 + p^2) + mx(\dot{r} + pq) + mz(rq - \dot{p}) + 2m(r\dot{x} - p\dot{z}) + m\ddot{y} \quad (4)$$

$$F_3 = m(\dot{w} + pv - qu) - mz(p^2 + q^2) + mx(pr - \dot{q}) + my(\dot{p} + rq) + 2m(p\dot{y} - q\dot{x}) + m\ddot{z} \quad (5)$$

The explanation of terms by grouping is as follows: first term is due to measurement of inertial velocity in a rotating frame; second, third, and fourth terms are due to coordinate system origin, not at the center of mass; fifth and sixth terms are due to relative velocity and acceleration of the mass center with respect to the coordinate system origin.

B. Moment Equations

Referring to Fig. 1, the moment about point O is

$$\mathbf{M}_o = \Sigma m_i \mathbf{r}_i \times \ddot{\mathbf{R}}_i \tag{6}$$

But, from Eq. (1),

$$\ddot{\mathbf{R}}_i = \ddot{\mathbf{R}}_o + [\ddot{\mathbf{r}}_i] + 2(\boldsymbol{\omega} \times [\dot{\mathbf{r}}_i]) + \boldsymbol{\omega} \times \mathbf{r}_i + \boldsymbol{\omega} \times (\boldsymbol{\omega} \times \mathbf{r}_i)$$

Substituting into (6),

$$\mathbf{M}_o = \Sigma m_i(\mathbf{r}_i \times \ddot{\mathbf{R}}_o) + \Sigma m_i \mathbf{r}_i \times [\ddot{\mathbf{r}}_i] + 2\Sigma m_i \mathbf{r}_i \times (\boldsymbol{\omega} \times [\dot{\mathbf{r}}_i]) + \Sigma m_i \mathbf{r}_i \times (\dot{\boldsymbol{\omega}} \times \mathbf{r}_i) + \Sigma m_i \mathbf{r}_i \times [\boldsymbol{\omega} \times (\boldsymbol{\omega} \times \mathbf{r}_i)] \tag{7}$$

Now, introducing the definition of moment of inertia for a rigid body with constant mass,

$$I_o \dot{\boldsymbol{\omega}} = \Sigma \mathbf{r}_i \times (\dot{\boldsymbol{\omega}} \times m_i \mathbf{r}_i) \tag{8}$$

$$\boldsymbol{\omega} \times I_o \boldsymbol{\omega} = \Sigma \mathbf{r}_i \times [\boldsymbol{\omega} \times m_i(\boldsymbol{\omega} \times \mathbf{r}_i)] \tag{9}$$

Substituting (8) and (9) into (7),

$$\mathbf{M}_o = m\mathbf{r} \times \ddot{\mathbf{R}}_o + \Sigma m_i \mathbf{r}_i \times [\ddot{\mathbf{r}}_i] + I_o \dot{\boldsymbol{\omega}} + \boldsymbol{\omega} \times I_o \boldsymbol{\omega} + 2\Sigma m_i \mathbf{r}_i \times (\boldsymbol{\omega} \times [\dot{\mathbf{r}}_i]) \tag{10}$$

Before substituting to obtain the three scalar moment equations, it is assumed that internal mass motion will occur only along a single body axis at any instant of time.

It is therefore assumed that $[\ddot{\mathbf{r}}_i]$ and $[\dot{\mathbf{r}}_i]$ are functions of time alone. Then one can write:

$$\sum_{i=1}^{m} m_i \mathbf{r}_i \times [\ddot{\mathbf{r}}_i] = -[\ddot{\mathbf{r}}_i] \times \sum_{i=1}^{p} m_i r_i$$

$$\sum_{i=p}^{m} m_i \mathbf{r}_i \times [\ddot{\mathbf{r}}_i] = 0 \tag{11}$$

$$2\Sigma m_i \mathbf{r}_i \times (\boldsymbol{\omega} \times [\dot{\mathbf{r}}]) = -(\boldsymbol{\omega} \times [\dot{\mathbf{r}}_i]) \times 2 \sum_{i=1}^{p'} m_i \mathbf{r}_i$$

$$\sum_{i=p}^{m} m_i r_i \times (\boldsymbol{\omega} \times [\dot{\mathbf{r}}']) = 0 \tag{12}$$

where p is the set of particles within the body with acceleration $[\ddot{\mathbf{r}}_i]$, and p' those with velocity $[\dot{\mathbf{r}}_i]$, respectively.

From the definition of the center of mass,

$$\sum_{i=1}^{m} m_i \mathbf{r}_i = m\mathbf{r}$$

Differentiating twice and noting $[\ddot{\mathbf{r}}_i]$ and $[\dot{\mathbf{r}}_i]$,

$$\sum_{i=1}^{p'} m_i[\dot{\mathbf{r}}_i] = m[\dot{\mathbf{r}}] \qquad [\dot{\mathbf{r}}_i] \sum_{i=1}^{p'} m_i = m[\dot{\mathbf{r}}]$$

$$\sum_{i=1}^{p} m_i[\ddot{\mathbf{r}}_i] = m[\ddot{\mathbf{r}}] \qquad [\ddot{\mathbf{r}}_i] \sum_{i=1}^{p} m_i = m[\ddot{\mathbf{r}}]$$

Substituting into (11) and (12),

$$\left[\sum_{i=1}^{p} m_i \mathbf{r}_i\right]\left[\sum_{i=1}^{p} m_i\right]^{-1} \times m[\ddot{\mathbf{r}}] = \mathbf{r}_A \times m[\ddot{\mathbf{r}}]$$

$$\left[2\sum_{i=1}^{p'} m_i \mathbf{r}_i\right]\left[\sum_{i=1}^{p'} m_i\right]^{-1} \times (\boldsymbol{\omega} \times m[\dot{\mathbf{r}}]) = 2\mathbf{r}_V \times (\boldsymbol{\omega} \times m[\dot{\mathbf{r}}])$$

where $\mathbf{r}_A$ is the vector from O to the centroid of the accelerating particles within the body, and $\mathbf{r}_V$ the corresponding vector to the centroid of the particles in motion. So Eq. (10) becomes

$$\mathbf{M}_o = m\mathbf{r} \times \ddot{\mathbf{R}}_0 + m\mathbf{r}_A \times [\ddot{\mathbf{r}}] + I_o \dot{\boldsymbol{\omega}} + \boldsymbol{\omega} \times I_o \boldsymbol{\omega} + 2m\mathbf{r}_V \times (\boldsymbol{\omega} \times [\dot{\mathbf{r}}]) \tag{13}$$

The explanation of terms by grouping is as follows: the first term is due to center of mass not coinciding with the body fixed origin; second term is due to internal mass acceleration; third and fourth terms are the change in angular momentum about O measured in a rotating frame of reference; and the fifth term is the Coriolis effect upon angular momentum caused by internal mass motion. The three scalar equations resulting from (13) are found by substituting the following quantities:

$$\dot{R}_o = u\boldsymbol{\alpha}_1 + v\boldsymbol{\alpha}_2 + w\boldsymbol{\alpha}_3 \qquad \boldsymbol{\omega} = p\boldsymbol{\alpha}_1 + q\boldsymbol{\alpha}_2 + r\boldsymbol{\alpha}_3$$

$$\mathbf{r} = x\boldsymbol{\alpha}_1 + y\boldsymbol{\alpha}_2 + z\boldsymbol{\alpha}_3 \qquad \dot{\mathbf{r}} = \dot{x}\boldsymbol{\alpha}_1 + \dot{y}\boldsymbol{\alpha}_2 + \dot{z}\boldsymbol{\alpha}_3$$

$$[\ddot{\mathbf{r}}] = \ddot{x}\boldsymbol{\alpha}_1 + \ddot{y}\boldsymbol{\alpha}_2 + \ddot{z}\boldsymbol{\alpha}_3 \qquad \mathbf{r}_A = x_A\boldsymbol{\alpha}_1 + y_A\boldsymbol{\alpha}_2 + z_A\boldsymbol{\alpha}_3$$

$$\mathbf{r}_V = x_V\boldsymbol{\alpha}_1 + y_V\boldsymbol{\alpha}_2 + z_V\boldsymbol{\alpha}_3$$

The moments of inertia will, in general, change because of mass movement. If the body is designed such that mass is transferred to symmetric positions with respect to point O along each of the body axes, and if the principal moments of inertia are evaluated at point O when it coincides with the center of mass, then the principal moments of inertia are invariant, and are $I_{xx_o} = I_{xx}$; $I_{yy_o} = I_{yy}$; and $I_{zz_o} = I_{zz}$; and the products of inertia can be expressed as functions of the displacement of the mass center from O: i.e., $I_{xy} = I_{xy}(x, y)$; $I_{xz} = I_{xz}(x, z)$; and $I_{yz} = I_{yz}(y, z)$. Substituting these quantities into (14),

$$M_x = I_{xx}\dot{p} - I_{xy}(\dot{q} - pr) - I_{xz}(\dot{r} + pq) + (I_{zz} - I_{yy})qr - I_{yz}(q^2 - r^2) + m(y\dot{w} - z\dot{v}) + my(pv - qu) - mz(ru - pw) + m(y_A\ddot{z} - z_A\ddot{y}) + 2my_V(p\dot{y} - q\dot{x}) + 2mz_V(p\dot{z} - r\dot{x}) \tag{14}$$

$$M_y = I_{yy}\dot{q} - I_{xy}(\dot{p} + qr) - I_{yz}(\dot{r} + qp) + (I_{xx} - I_{zz})pr - I_{xz}(r^2 - p^2) + m(z\dot{u} - x\dot{w}) + mz(qw - rv) - mx(pv - qu) + m(z_A\ddot{x} - x_A\ddot{z}) + 2mz_V(q\dot{z} - r\dot{y}) + 2mz_V(q\dot{x} - p\dot{y}) \tag{15}$$

$$M_z = I_{zz}\dot{r} - I_{xz}(\dot{p} - qr) - I_{yz}(\dot{q} + pr) + (I_{yy} - I_{xx})pq - I_{xy}(p^2 - q^2) + m(x\dot{v} - y\dot{u}) + mx(ru - pw) - my(qw - rv) + m(x_A\ddot{y} - y_A\ddot{x}) + 2mx_V(r\dot{x} - p\dot{z}) + 2my_V(r\dot{y} - q\dot{z}) \tag{16}$$

Equations (3–5 and 14–16) represent the general kinematic expressions for a six-degree-of-freedom body with internal mass movement.

The hydrodynamic loads acting on the vehicle are given by

$$(F_1)_{\text{hyd}} = \frac{\rho l^4}{2}[X'_{qq}q^2 + X'_{rr}r^2 + X'_{rp}rp] + \frac{\rho l^3}{2}[X'_{\dot{u}}\dot{u} + X'_{vr}vr + X'_{wq}wq] + \frac{\rho l^2}{2}[X'_{u|u|}u^2 + X'_{vv}v^2 + X'_{ww}w^2] \tag{17}$$

$$(F_2)_{\text{hyd}} = \frac{\rho l^4}{2}[Y'_{\dot{r}}\dot{r} + Y'_{\dot{p}}\dot{p}] + \frac{\rho l^4}{2}Y'_{pq}pq + \frac{\rho l^3}{2}[Y'_{\dot{v}}\dot{v} + Y'_{wp}{}^2wp] + \frac{\rho l^3}{2}[Y'_{ur}ur + Y'_{|v|r}|v|r + Y'_{up}up] + \frac{\rho l^2}{2}[Y_*u^2 + Y'_{vu}uv + Y'_{v|v|}v|v|] + \frac{\rho l^2}{2}u^2Y'_{\delta r}\delta r + \frac{\rho l^2}{2}u^2Y'_{\delta r|\delta r|}\delta r|\delta r| \tag{18}$$

$$(F_3)_{hyd} = \frac{\rho l^4}{2}[Z'_{\dot{q}}\dot{q} + Z'_{rr}r^2] + \frac{\rho l^3}{2}[Z'_{\dot{w}}\dot{w} + Z'_{vp}vp + Z'_{Vr}Vr] + \frac{\rho l^3}{2}[Z'_{q}uq + Z_{|w|q}|w|q] + \frac{\rho l^2}{2}[Z'_{*}u^2 + Z'_{w}uw + Z'_{w|w|}w|w|] + \frac{\rho l^2}{2}u^2Z'_{\delta s}\delta_s + \frac{\rho l^2}{2}u^2Z_{\delta s|\delta s|}\delta s|\delta s| \quad (19)$$

$$K = \frac{\rho l^5}{2}[K'_{\dot{p}}\dot{p} + K'_{qr}qr + K_{\dot{r}}\dot{r} + K_{p|p|}p|p|] + \frac{\rho l^4}{2}[K'_{p}up + K'_{r}ur + K'_{\dot{v}}\dot{v}] + \frac{\rho l^3}{2}\times [K'_{*}u^2 + K'_{v}uv + K'_{v|v|}v|v| + K'_{vw}vw] \quad (20)$$

$$M = \frac{\rho l^5}{2}[M'_{\dot{q}}\dot{q} + M'_{rp}rp] + \frac{\rho l^4}{2}[M'_{q}uq + M'_{w|q|}|w|q] + \frac{\rho l^3}{2}[M'_{*}u^2 + M'_{w}uw + M'_{w|w|}w|w|] + \frac{\rho l^3}{2}[M'_{vv}v^2] + \frac{\rho l'}{2}M'_{vr}vr + \frac{\rho l^5}{2}M'_{rr}r^2 + \frac{\rho l^4}{2}M'_{\dot{w}}\dot{w} + \frac{\rho l^3u^2}{2}[M'_{\delta s}\delta_s] + \frac{\rho l^3}{2}u^3[M'_{\delta s|\delta s|}\delta s|\delta s|] \quad (21)$$

$$N = \frac{\rho l^5}{2}[N'_{\dot{r}}\dot{r} + N'_{pq}pq + N'_{\dot{p}}\dot{p}] + \frac{\rho l^4}{2}\times [N'_{r}ur + N'_{|v|r}|v|r] + \frac{\rho l^4}{2}[N'_{p}up + N'_{\dot{v}}\dot{v}] + \frac{\rho l^3}{2}[N'_{*}u^2 + N'_{v}uv + N'_{v|v|}v|v|] + \frac{\rho l^3u^3}{2}[N'_{\delta r}\delta r + N'_{\delta r|\delta r|}\delta r|\delta r] \quad (22)$$

The body forces and moments are obtained as follows:

$$(W - B)k = -(W - B)(\sin\theta)\boldsymbol{\alpha}_1 + (W - B)(\cos\theta\sin\varphi)\boldsymbol{\alpha}_2 + (W - B)(\cos\theta\cos\varphi)\boldsymbol{\alpha}_3$$

The corresponding moments are

$$\mathbf{M}_o = \mathbf{r} \times \mathbf{W} + \mathbf{r}' \times \mathbf{B} \quad (23)$$

$$\mathbf{M}_o = [(Wy - By_B)\cos\theta\cos\varphi + (Bz_B - Wz)\cos\theta\sin\varphi]\boldsymbol{\alpha}_1 + [(Bz_B - Wz)\sin\theta + (Bx_B - Wx)\cos\theta\cos\varphi]\boldsymbol{\alpha}_2 + [(Wx - Bx_B)\cos\theta\sin\varphi + (Wy - By_B)\sin\theta]\boldsymbol{\alpha}_3$$

Equations (17–23) describe the hydrodynamic forces and torques exerted on the vehicle as well as the forces and moments acting on the vehicle due to the buoyancy of the vehicle. The hydrodynamic coefficients are known only for the conditions where the forward velocity is the dominant motion of the vehicle. For this condition, many of the hydrodynamic terms can be neglected.

The six equations that describe the vehicle and contain the most significant terms are as follows:

Surge

$$m[\dot{u} + qw - rv + \ddot{x}] = \frac{\rho l^3}{2}[X'_{\dot{u}}\dot{u} + X'_{vr}vr + X'_{wq}wq] + \frac{\rho l^2}{2}X'_{uu}u^2 - [(W - B)\sin\theta + F_x \quad (24)$$

Sway

$$m[\dot{v} + ru - pw + \ddot{y}] = \frac{\rho l^4}{2}Y'_{\dot{r}}\dot{r} + \frac{\rho l^3}{2}[Y'_{\dot{v}}\dot{v} + Y'_{p}up + Y'_{wp}wp + Y'_{r}ur] + \frac{\rho l^2}{2}Y'_{v}uv + \frac{\rho l^2}{2}[Y_{*}u^2 + Y'_{v|v|}v|v] + \frac{\rho l^2}{2}u^2Y'_{\delta r}\delta r + \frac{\rho l^2}{2}u^2Y'_{\delta r|\delta r|}|\delta r|\delta r + (W - B)\cos\theta\sin\varphi + F_y \quad (25)$$

Heave

$$m[\dot{w} + pv - qu] = \frac{\rho l^4}{2}Z'_{\dot{q}}\dot{q} + \frac{\rho l^3}{2}[Z'_{\dot{w}}\dot{w} + Z'_{q}uq + Z'_{vp}vp] + \frac{\rho l^2}{2}[Z'_{*}u^2 + Z'_{w}uw + Z'_{w|w|}w|w] + \frac{\rho l^2}{2}u^2Z'_{\delta s}\delta s + \frac{\rho l^2}{2}u^2Z'_{\delta s|\delta s|}\delta s|\delta s| + (W - B)\cos\theta\cos\varphi + F_z \quad (26)$$

Roll

$$\mathbf{I}_{xx}\dot{p} + (\mathbf{I}_{zz} - \mathbf{I}_{yy})qr - myqu = \frac{\rho l^5}{2}K'_{\dot{p}}\dot{p} \frac{\rho l^4}{2}[K'_{r}ur + K'_{\dot{v}}\dot{v}] + \frac{\rho l^3}{2}K'_{v}uv + \frac{\rho l^4}{2}K'_{p}up - Wy\cos\theta\cos\varphi + BZ_B\cos\theta\sin\varphi + \Sigma K \quad (27)$$

Pitch

$$\mathbf{I}_{yy}\dot{q} + (\mathbf{I}_{xx} - \mathbf{I}_{zz})pr + mxqu = \frac{\rho l^5}{2}[M'_{\dot{q}}\dot{q} + M'_{rp}rp] + \frac{\rho l^4}{2}M'_{\dot{q}}uq + \frac{\rho l^3}{2}[M'_{*}u^2 + M'_{w}uw + M'_{w|w|}ww|] + \frac{\rho l^4}{2}[M'_{\dot{w}}w] + \frac{\rho l^3}{2}u^2M'_{\delta s}\delta_s + BZ_B\sin\theta - Wx\cos\theta\cos\varphi + \Sigma M + \frac{\rho l^3}{2}u^2M'_{\delta s|\delta s|}\delta|\delta| \quad (28)$$

Yaw

$$\mathbf{I}_{zz}\dot{r} + (\mathbf{I}_{yy} - \mathbf{I}_{xx})pq + mxru = \frac{\rho l^5}{2}[N'_{\dot{r}}\dot{r} + N'_{pq}pq] + \frac{\rho l^4}{2}[N'_{r}ur + N'_{\dot{v}}\dot{v}] + \frac{\rho l^4}{2}[N'_{p}up] + \frac{\rho l^3}{2}[N'_{v}uv + N'_{*}u^2 + N'_{v|v|}v|v + N'_{\delta r}u^2\delta r + N'_{\delta r|\delta r|}u^2\delta r|vr|] + Wx\cos\theta\sin\varphi + Wy\sin\theta + \Sigma N \quad (29)$$

Attitude Stability and Control

In the preceding section, the general six-degree-of-freedom equations were developed where the forward velocity was the predominant motion of the vehicle. In this section, the simplified roll characteristics of the vehicle are used to investigate the feasibility of controlling the vehicle attitude by pumping mercury from tank to another inside the vehicle. Although only roll control is considered here, this control scheme is equally applicable to pitch control. The complete six-degree-of-freedom equations were simulated on an analog computer and the results of this simulation for roll commands are included here to verify the simplified roll loop analysis.

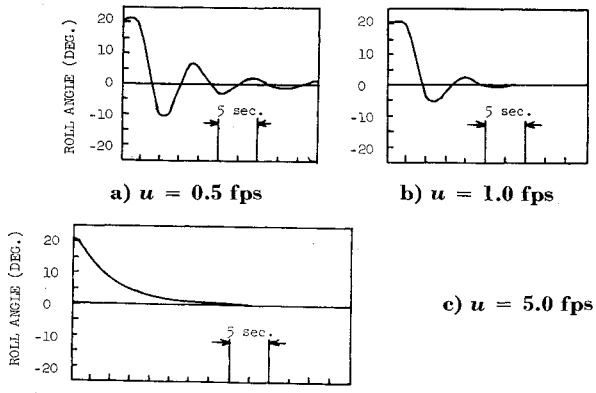

Fig. 2 Roll response of the DSRV to an initial roll angle of 20°.

A. Roll Stability and Control

The simplified roll transfer function from motion of the center of mass along the y axis to roll angle used here is given by

$$\varphi/y = W/(b_1 s^2 + b_2 us + b_3) \tag{30}$$

where

$$b_1 = \mathbf{I}_{xx} - \frac{\rho l^5}{2} K'_{\dot{p}} \qquad b_2 = -\frac{\rho l^4}{2} K'_p \qquad b_3 = -BZ_B$$

This is just the roll transfer function when the vehicle is constrained to one degree of freedom (roll) at a constant forward velocity. An examination of the magnitude of the coefficients for various cross-coupling terms (see Ref. 1) as well as the close agreement between the roll step response for the exact and the simplified roll transfer functions justify using the simplified roll transfer function for preliminary design purposes. The approximate roll natural frequency is given by

$$W_n^2 = \frac{-BZ_B}{I_{xx}(-\rho l^5/2)K'_{\dot{p}}}$$

and the damping ratio given by

$$DR = (-\rho l^4 K'_p/4W_n)u$$

If the buoyancy force and metacentric height remain constant, then the natural frequency of the vehicle is invariant for all forward velocities and the damping ratio is linearly dependent upon the forward velocity. At low forward velocities, the simplified roll transfer function is no longer valid since many of the cross-coupling terms become more significant and cause additional damping or roll disturbances. In a sense, the simplified roll transfer function is worse than the actual roll transfer function since some of the natural roll damping is being neglected. Figure 2 shows the roll response of the vehicle to an initial roll angle of 20 deg as the forward velocity is changed from 0.5 to 5.0 fps.

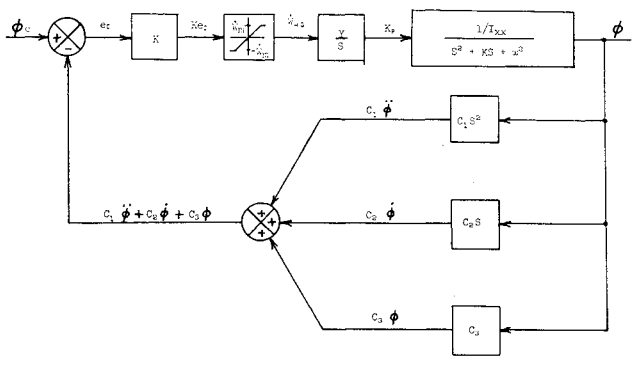

Fig. 3 Simplified mathematical block diagram for the DSRV roll control system.

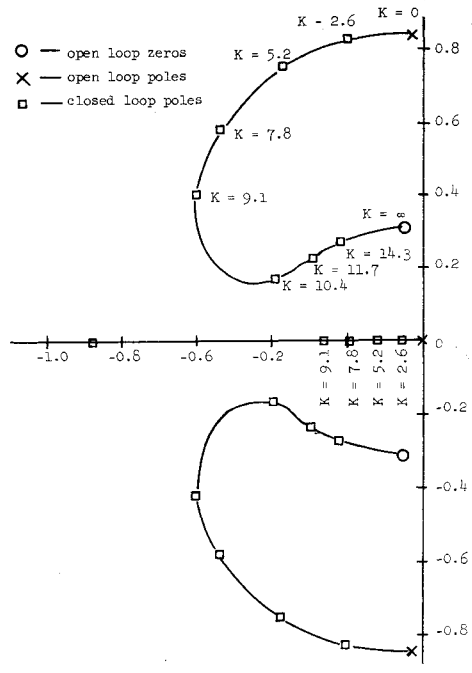

Fig. 4 Root locus for simplified roll control system; $\theta_f = 10\,\ddot{\theta} + \dot{\theta} + \theta$; u = 0.1 fps; maximum mercury flow rate = 40 lb/sec.

For low velocities (Fig. 2a), the roll response is lightly damped and requires many oscillations before the roll motion is completely damped out. For large forward velocities (Figs. 2b and 2c), the roll damping increases until the response is overdamped and asymptotically approaches a final value. The most critical roll control requirements are during the mating process when the forward velocity is very small. The roll response of the vehicle during this mating process is unacceptable and some means of improving the roll response at low velocities must be used.

Similarly, the least critical roll control requirements are during the cruise mode when the forward velocity of the vehicle is large. For large forward velocities, the natural roll response of the vehicle is acceptable so that a closed-loop roll control system is not required in the cruise mode.

Closed-loop roll control is accomplished by using the mercury trim system to change the center of mass along the y axis of the vehicle, and, consequently, to provide torques about the roll axis. The change in y due to moving mercury along the vehicle y axis can be determined from the definition of center of mass;

$$y = \int y_i m_i/m \tag{31}$$

For the mercury trim system

$$Wy = \int W_{\mathrm{Hg}} y_i dt$$

where y_i = distance that mercury is moved, and $\dot{W}_{\mathrm{Hg}}$ = mercury flow rate in lb/sec.

The Laplace transform of this equation is

$$Wy = (1/s)\dot{W}_{\mathrm{Hg}} y_i \tag{32}$$

so that

$$\varphi/\dot{W}_{\mathrm{Hg}} = y_i/s(b_1 s^2 + b_2 us + b_3) \tag{33}$$

For the DSRV, y_i is the distance between the two mercury tanks located on the y axis and is 6.67 ft.

A simplified mathematical model of the closed-loop roll control system is shown in Fig. 3. The mercury trim sys-

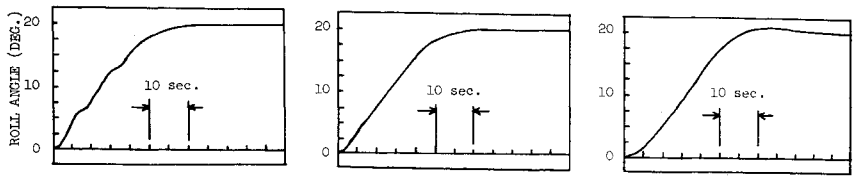

Fig. 5 Step response of the DSRV with the closed-loop control system operative; maximum mercury flow rate = 40 lb/sec.

a) u = 0.1 fps **b) u = 1.0 fps** **c) u = 5.0 fps**

tem is shown as an integrator and the valve that controls the flow of the mercury is represented as linear till it reaches saturation at the maximum flow capacity of the valve.

If just the linear portion of the valve is first considered, then the required compensation for the roll control can be determined by the usual linear compensation techniques. Figure 4 shows the root locus of the roll control system (u = 0.1 fps) when the feedback signal is $\varphi_x = 10\ddot{\varphi} + \dot{\varphi} + \varphi$. As the gain K is increased, the closed-loop poles move such that their damping is increased. When $K = 10$, the damping ratio is approximately 0.9. For this damping ratio, the DSRV roll step response will have no overshoot. This is especially important during the docking maneuver when the pilot is trying to orient the DSRV so that the skirt mating surface is parallel to the mating surface on the target sub.

Figure 5 compares roll step responses for a 20° step input at three forward velocities. For u = 0.1 fps, there is no overshoot and the rise time is 35 sec. When the forward velocity is increased to 1.0 fps, the roll response remains virtually unaffected, and when the forward velocity is increased to 5.0 fps, the compensated roll control system response has an overshoot of about 10%. Figure 5 shows the roll response when the forward velocity is 5 fps. However, at forward velocities greater than 1.0 fps the roll response is not as critical as during the mating process when the forward velocity is nearly 0, and, at large forward velocities, the open-loop vehicle roll characteristics are acceptable and the closed-loop control system need not be used.

For a small command signal, the mercury flow rate does not saturate and the roll control system is a linear system. For larger command signals, the mercury flow rate saturates and the roll response of the vehicle is altered. Figure 6 compares the response of the vehicle to a step input of 8 deg and with the vehicle response to a step input of 40 deg. Figure 6a shows the response of the vehicle to an 8-deg step input when the mercury flow rate does not saturate. The rise time is approximately 35 sec. In Fig. 6b, the mercury flow rate is saturated during the first part of the step response so that the torque applied to the vehicle is a ramp (integral of the constant torque rate). The first portion of the response is the open-loop response to a ramp input. Since the natural damping of the vehicle is small for low velocities, the vehicle response to the ramp input is oscillatory. After approximately 45 sec, the mercury flow rate is no longer saturated and the vehicle response becomes more heavily damped. The rise time for the 40° step input is 60 sec.

The rise time for a roll step response depends on the maximum mercury flow rate. Figure 6a showed the roll step response where the maximum mercury flow rate was 40 lb/sec. Shorter step response times could be achieved by increasing the mercury flow rate, although satisfactory roll response can be obtained with a maximum mercury flow rate less than the 40 lb/sec used in Fig. 6a. In general, the maximum flow rate should be selected on the basis of roll rise time requirements.

In Fig. 7, the roll responses for the closed-loop roll control system and the open-loop control system for the vehicle are compared for a 100 ft-lb roll disturbance torque. Figure 7a shows the open-loop roll response to the disturbance torque. The response takes more than 80 sec to die out, and the final roll angle is changed to 3 deg. The peak roll angle is 5.8 deg. The closed-loop disturbance response, shown in Figure 7b, takes 25 sec to damp out, has a peak roll angle of 2.0 deg and the original steady-state roll angle is not changed. This is very important when the vehicle is trying to mate with the target submarine.

To verify that the roll control analysis using the simplified roll transfer function did give valid results, the full six-degree-of-freedom equations were simulated on an analog computer. The mercury trim system and the roll control system developed in the simplified analysis were also simulated. The vehicle response to step roll commands is shown in Fig. 8 for two different nominal vehicle forward velocities and nominal pitch angles. The roll response of the complete six-degree-of-freedom simulation is nearly identical to the results predicted by the simplified roll analysis. Reference 4 contains a complete summary of the control system development for all six degrees of freedom of the DSRV, using an analog computer simulation.

Physical Realization of Mercury Trim System

The roll error signal that actuates the valve solenoid causes mercury to flow in the proper direction to provide a roll torque on the vehicle. This torque acts on the DSRV to roll the vehicle to the desired attitude in an acceptable manner. One method of transporting mercury from one roll tank to the other to provide roll torques is shown in Fig. 9. The system consists of a motor and a hydraulic pump which supplies a hydraulic pressure of 500 psi. The output of the pump is used to charge a gas accumulator whose working volume is equal to the volume of one of the trim tanks. Each trim tank is separated into two separate halves by an elastic bladder with the bottom half of each trim tank connected by a pipe allowing mercury to flow from one trim tank to the other. The total volume of mercury contained in the system is equal to the volume of one sphere plus the volume of the pipe connecting the two trim tanks. This allows one trim tank to be completely full of mercury when the other tank is empty of mercury.

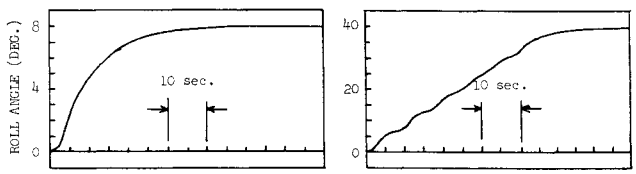

a) 8° roll step response **b) 10° roll step response**

Fig. 6 DSRV roll response with u = 0.1 fps; maximum mercury flow rate = 40 lb/sec.

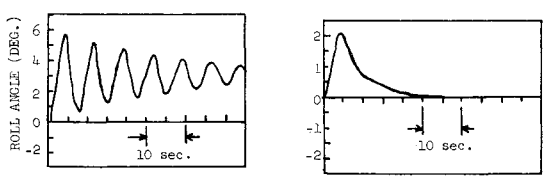

a) Open loop **b) Closed loop**

Fig. 7 Roll disturbance response.

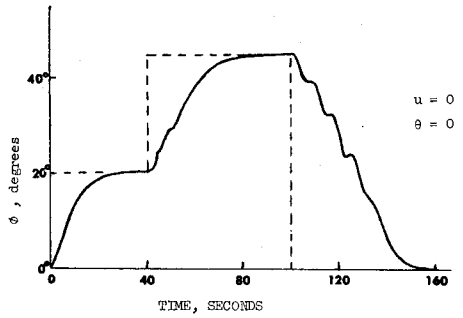

Fig. 8 Roll responses; --- step command; ω_{Hg} = 50 lb/sec max; BG = 2 in.

The upper portions of each trim tank are connected to the hydraulic accumulator through the 4-way valve. To move mercury from one trim tank to the other, the valve solenoid moves the valve spindle so that one trim tank is connected to the accumulator while the other trim tank is connected to the vent tank. This causes hydraulic fluid to flow into one trim tank and out of the other, and, consequently, for mercury to flow from one tank to the other. The mercury flow rate depends on the valve displacement, the pressure of the accumulator, pipe friction, and vehicle roll angle. The approximate time required for the mercury flow rate to reach a maximum can be computed by considering the time required for mass in the pipe to reach the desired flow rate when the accumulator pressure is 500 psi.

The equation of motion of the mercury in the pipe is

$$(\delta P)(A) - \gamma A(z_1 - z_2) + \gamma AL \sin\varphi - \frac{\gamma AfL}{2gD}\left(\frac{dz}{dt}\right)^2 = \frac{\gamma AL}{g}\frac{d^2z}{dt^2} \quad (34)$$

The individual terms are defined as follows: first term, external pressure load applied from the accumulator; second, external forces caused by the mercury in the reservoir on the mercury in the pipe; third, viscous fluid resistance in the pipe, and fourth inertia of the mercury in the pipe. The equation is nonlinear because of the presence of $(dz/dt)^2$. Examination of the Reynolds number for mercury in a 1-in.-diam pipe with flow rate of 40 lb/sec, shows that $R_e < 0.5 \times 10^6$. Assuming these values the viscous forces can be neglected, i.e., $\gamma A(z_1 - z_2) + \gamma AL \sin\varphi \gg (\gamma AfL/2gD)\text{-}(dz/dt)^2$ for most realistic roll angles. Then $(\delta P)(A) - \gamma A(z_1 - z_2) + \gamma AL \sin\varphi = (\gamma AL/g)(d^2z/dt^2)$. z_1 and z_2 are the equivalent mercury displacements in the reservoir tanks, assuming the mercury incompressible; $Az = A'z_1 = -A'z_2$ where A' is the reservoir cross-sectional area. Substituting in (34), the equation of motion for the mercury is

$$\ddot{z} + (2g/L)(A/A')Z = g\delta P/\gamma L + g\sin\varphi \quad (35)$$

It should be noted that the δP from the accumulator acts such that $\delta P > Oz > 0$ and $\delta P < O < 0$. Then subject to these restrictions, and letting $\Omega_N^2 = (2g/L)(A/A') = \text{const}$, for $\delta P > 0$,

$$z(t) = \tfrac{1}{2}(A'/A)(\delta P/\gamma) + (L\sin\varphi)(1 - \cos\Omega_N t) \quad (36)$$

where $\dot{z} > 0$ and

$$\dot{W}_{Hg} = \gamma A\dot{z} = [(g/2L)AA']^{1/2}(\delta P + \delta L \sin\varphi)\sin W_N t$$

The necessary assumption to arrive at the preceding solution required that the vehicle roll angle remain constant during acceleration. This condition can be shown to be satisfied by examining $\dot{W}_{Hg}(t_1, \delta P)$. For $\delta P \gg \delta L \sin\varphi$, $W_{Hg}(t, \delta P) = [\text{const}]\ \delta P \sin\Omega_N t$ (see Fig. 10). For a maximum flow rate of $\dot{W}_o$, the δP design pressure can be sized according to the maximum allowable time lag for reaching maximum rate flow. The worst case (i.e., where time to reach $\dot{W}_o$ is reached) is

$$t_M = \frac{1}{\Omega_N}\sin^{-1}\left(\frac{\dot{W}_o}{\delta P}\left[\frac{g}{2L}AA'\right]^{-1/2}\sec\frac{\pi}{4}\right) \quad (37)$$

For $A = (\gamma/576)\text{ft}^2$, $A' = 0.16\pi$ ft^2, $L = 6.67$, $W_o = 40$ lb/sec, $\delta P = 500$ psi, and [$t_m = 0.0356$ sec].

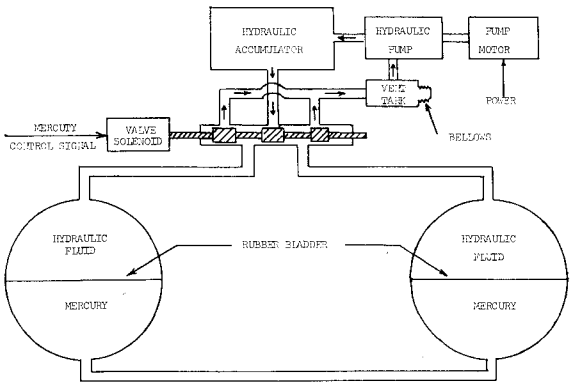

Fig. 9 Mercury trim system for roll control.

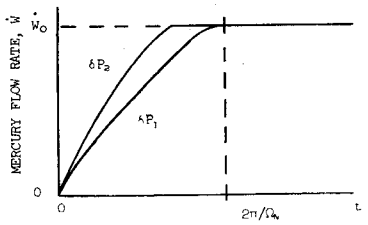

Fig. 10 Flow rate response of the mercury transfer system.

References

[1] Martin, M. and Goodman, A., "Equations of Motion and Some Preliminary Estimated Coefficients for BuShips Rescue I," T.M. 511-1, Jan. 1965, Hydronautics Inc.

[2] Bell, H. E. et al., "A Geometrical Analysis of Several Techniques to Aid in Effecting a Mate between the DSRV and a Target Submarine," TR-801, April 1966, Naval Avionics Facility, Indianapolis, Ind.

[3] Palamara, R. D., "An Investigation of Optimal Paths through Perturbing Flow Fields for the DSRV," TR-900, Sept. 1966, Naval Avionics Facility, Indianapolis, Ind.

[4] Bridges, W. J., "Summary of DSRV Control System Design and Simulation," TR-867, Aug. 1966, Naval Avionics Facility, Indianapolis, Ind.

Bibliography

Palamara, R. D., "Equations of Motion of a Deep Submergence Rescue Vehicle with Variable Center of Mass," TR-638, Aug. 1965, Naval Avionics Facility, Indianapolis, Ind.

Bridges, W. J., "Attitude Control of a Deep Submergence Rescue Vehicle," TR-710, Nov. 1965, Naval Avionics Facility, Indianapolis, Ind.

Snare, L. E., "Description of a Control System for a Deep Submergence Rescue Vehicle," TR-768, Jan. 1966, Naval Avionics Facility, Indianapolis, Ind.

Palamara, R. D. and Bridges, W. J., "DSRV Shroud-Actuator Equations of Motion," TR-779, Feb. 1966, Naval Avionics Facility, Indianapolis, Ind.